
FINDING THE TRIGGER: CAUSAL ABDUCTIVE REASONING ON VIDEO EVENTS

Thao Minh Le¹, Vuong Le², Kien Do¹, Sunil Gupta¹, Svetha Venkatesh¹, Truyen Tran¹

¹Applied Artificial Intelligence Institute, Deakin University, Australia

²Amazon, Melbourne, Australia

{thao.le,k.do,sunil.gupta,svetha.venkatesh,truyen.tran}@deakin.edu.au
levuong@amazon.com

ABSTRACT

This paper introduces a new problem, Causal Abductive Reasoning on Video Events (CARVE), which involves identifying causal relationships between events in a video and generating hypotheses about causal chains that account for the occurrence of a target event. To facilitate research in this direction, we create two new benchmark datasets with both synthetic and realistic videos, accompanied by trigger-target labels generated through a novel counterfactual synthesis approach. To explore the challenge of solving CARVE, we present a Causal Event Relation Network (CERN) that examines the relationships between video events in temporal and semantic spaces to efficiently determine the root-cause trigger events. Through extensive experiments, we demonstrate the critical roles of event relational representation learning and interaction modeling in solving video causal reasoning challenges. The introduction of the CARVE task, along with the accompanying datasets and the CERN framework, will advance future research on video causal reasoning and significantly facilitate various applications, including video surveillance, root-cause analysis and movie content management.

1 Introduction

Modern AI research has achieved unprecedented progress in exploring statistical patterns from massive amounts of data to infer knowledge about the world. This is often referred to as inductive reasoning. For many inductive reasoning tasks, AI systems have already outperformed humans, such as image recognition [1] and voice recognition [2]. However, while humans excel at generating hypotheses and intuitions about the *causes of an observation*, this capability remains a blind spot for AI systems. For example, current medical AI systems are trailing behind human doctor in determining the probable cause of a disease diagnosis from patient’s medical history, lifestyle and their recent travel history. This type of inference is called *Abductive reasoning* and was first introduced by Charles Sanders Peirce [3]. In the field of video analysis, this fundamental problem translates into important and impactful requirement of finding the cause-effect pairs of events within the video.

Aiming at this problem, this paper studies a new task called *Causal Abductive Reasoning on Video Events* (CARVE) requiring AI systems to comprehend the causal relations embedded in the videos at the *event level* and generate hypotheses about the *trigger event* - a prior event in the video that most probably caused the occurrence of a query *target event*. CARVE promises significant breakthrough in numerous applications. For instance, in video surveillance, CARVE can help trace back the causal chain of a suspicious behavior to see why it was anomalous; in sports analysis, the task supports analyzing an unexpected move of a player on the field and suggest the likely reason such as a change in strategy or an injury; in movie production, the storyline of long videos can be broken down to identify illogical or redundant parts and provide suggestions for edition.

Along with proposing the CARVE task, we introduce two benchmark datasets built with counterfactual synthesis through interventional schemes. The first one is the namesake CARVE dataset featuring noise-free videos of dynamic objects that are created through a physics simulator. The trigger-target labels are generated by counterfactual video

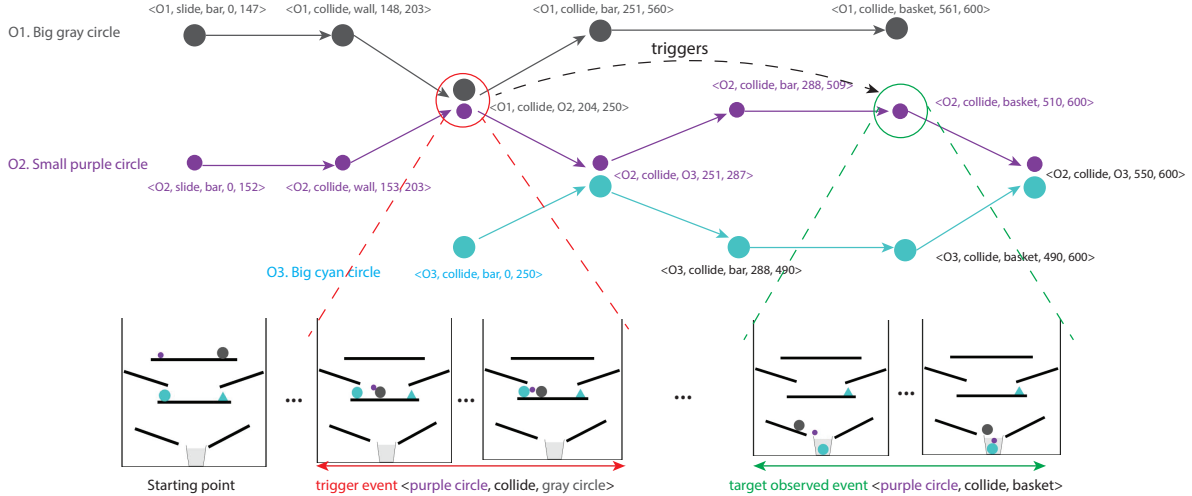


Figure 1: Illustration of event chains and trigger-target event pairs in CARVE task and example in the accompanying dataset. Videos are generated by a 2D physics simulator using predefined visual scenes. Video events, $\langle object_id_1, object_id_2, interaction_type, start_time, end_time \rangle$, are defined as interactions between a dynamic object and an object partner within a time interval. Each dynamic object creates a chain of events (3 in this example, marked with corresponding colors). These chains are merged by mutual events, resulting in a graph of events. Explanation and target event pairs are identified by comparing the original video and counterfactual videos. Best viewed in color.

generation. The second dataset *EpicKitchen-AR* leverages the realistic videos from action forecasting task in the EpicKitchen dataset and augment them with abductive events labels, also through counterfactual synthesis. Figure 1 illustrates the CARVE task and an example of the datasets.

Attempting at solving the new challenge, we propose a novel *Causal Event Relation Networks (CERN)*. The method focuses on modeling both temporal dependencies and semantic dependencies between video events toward finding their trigger-target relationships. CERN has this done by building a temporal-constrained directed event graph network built on input event features. The framework is generic to a variety of event feature representations demonstrated with its performance on both synthetic CARVE and the lifelike EpicKitchen-AR data.

Extensive experiments on the two datasets indicate that the task introduces a new distinctive challenge to video understanding field, demonstrated on the fact that fine-tuned large-scale video recognition models, such as MVITv2 [4], and powerful large video-language models such as Video-LLaVA [5] all fall short in this new task, due to their inability to disentangle the event causal relations with other types. The experiments also show the advantages of the new proposed method CERN against various baseline methods and suggest promising directions for the task.

Overall, this work aims at initiating a research topic of causal abductive reasoning for video events and makes three contributions: (1) Proposing a new task CARVE and building two rich and diverse datasets using counterfactual synthesis (2) A novel neural framework for event-graph modeling toward effectively solving CARVE task and (3) Extensive experiments that reveal the challenges of the task and indicate directions for development in this new front.

2 Related Work

Visual Abductive (VA) reasoning: This task is traditionally formulated as question-answering [6, 7, 8, 9] where the cause of an event is selected from multiple choices annotated by human. Another line of works approach abductive reasoning in the form of linguistic explanations [10, 11, 12, 13, 14] with strong reliance on textual captioning. The concrete trigger-target pair settings make CARVE distinctive from these work that aims at generating a generic hypothetical explanation that only might be associated with an actually happened event. Furthermore, this new task requires the focus on spatio-temporal visual properties and avoid linguistic bias and ambiguity, therefore making it closer to the targeted applications. Our work also transcend from visual reasoning about object’s relations and physics [15, 16, 17, 18, 8] by extending to life-like video events.

Visual Abductive datasets: Currently available VA datasets, including VAR [10], CLEVRER family [8, 19] are all based on artificial explanation generated by either human annotations which are subjective to human annotators or

preset written scripts which are biased to linguistic commonsense. To aim at more genuine visual casual data, we break this tradition with a new counterfactual synthesis procedure to reconstruct the objective cause-effect facts.

Event-relation modeling: Previous works focus on event localization [20, 21, 22] and video future events predictions [23, 24]. Structured representations of events are popular for these problem with action scene graphs [25] and action role labels [26]. Event-level graph in our work are built on top of the recent progress in video spatio-temporal graph models such as unified video-text event graph [27] and pseudo-3D scene graph [6]. The event-related applications recently saw further progress with vision transformer-based methods [28, 29, 4], however, video causal reasoning remains a challenge, especially at event level.

Generic abductive reasoning: Outside of computer vision, abductive reasoning has been explored using event calculus and temporal action logic [30]. In linguistics, abduction for text-based events in commonsense narrative contexts is collected and labeled by human labors [31]. It is also explored in medical diagnosis [32] and root-cause-analysis [33]. These works give insight and ideas to the new abductive reasoning task using causal relation of video events introduced in this paper.

3 Causal Abductive Reasoning on Video Events

3.1 Task Definition

The Causal Abductive Reasoning on Video Events (**CARVE**) involves analyzing a sequence of chronological events to identify preceding events that contributed causally to the occurrence of a target event. Here, we consider CARVE in the video understanding context. Specifically, within a sequence of events found in a video, we consider a **target event** at position N : $e^{\text{target}} = e_N$. The CARVE asks AI systems to find all the ground-truth trigger events E^{trigger} within the set of premise events $E^{\text{premise}} = \{e_1, \dots, e_{N-1}\}$ that are the causal reasons of the target. This setting excludes the case where $E^{\text{trigger}} = \emptyset$, meaning the target is an exogenous event triggered by factors outside of the video. We treat our CARVE as a binary classification problem where $y_i = 1$ indicates that a preceding event e_i is a cause of e^{target} and $y_i = 0$ otherwise. Formally, our task is to maximize the probability that an event $e_i \in E^{\text{trigger}}$ is correctly identified as a trigger event for the target event:

$$\theta^* = \operatorname{argmax}_{\theta} \sum_{e_i \in E^{\text{premise}}} P_{\theta}(y = 1 | e_i, e^{\text{target}}, E^{\text{premise}}), \quad (1)$$

where θ indicates model parameters.

This task is different from the previous visual abductive reasoning tasks by raising the requirement that the *causing factor must be grounded into a subset of premise events* instead of as generic textual description of the cause either in free form [10] or QA [8, 19] formats. This requirement bring the task closer to a large set of applications where the root cause needs to be traced back to previous video events.

3.2 Counterfactual Causal Event Datasets

The top challenge for observational models for causal discovery tasks like CARVE is to separate causal relations with associative biases. For example, “eating ice cream” is usually associated with “sun burnt” while actually caused by “hot weather”. This separation theoretically requires training and evaluation data *with ground truth cause-effect pairs discovered with interventional experiments* [34]. Traditionally, these interventions are estimated by randomized controlled trials but they are universally costly and mostly infeasible for life-like video events. This challenge in building causal data encouraged a popular alternative direction where the event causes are specified as *linguistic explanations* learned from causal facts extracted from literature corpus [10]. Another work around is through human annotation, either in explanation form or in question-answering format [8, 19]. While avoiding the roadblock, these datasets are prone to diverging from the true causal relation between events, often leaning on linguistic causal commonsense provided by explanatory generative models - which are overly smooth or human annotator who can be objective and inconsistent. For example, while “eating ice cream” is commonly explained by “hot weather”, in a particular video, it can be actually caused by the real event of “attending a birthday party”.

To break through these limitations, we propose to directly address interventional data generation by using counterfactual synthesis where the candidate trigger events are one-by-one omitted from the video to observe its consequential role to the target event. This approach helps establish two video event datasets as benchmark for the CARVE task: The CARVE dataset produced using a fully controlled 2D physics simulator, and the realistic *EpicKitchen-AR* leverages the real-world scenarios using life-like videos extracted from the popular EpicKitchen-100 dataset. Meanwhile, the *EpicKitchen-AR* set ensures the practicality in dealing with lifelike videos.

Algorithm 1 Abductive Event Pairs Extraction

Input: \mathcal{G} : Event graph of the input video
 e_t^{target} : target event of main object t
 C : counterfactual dynamic objects of e_t^{target}
Output: H : List of trigger events for e_t^{target}

- 1: Initialize $H \leftarrow \{\}$
- 2: **for each** $c \in C$ **do**
- 3: $e_c^{\text{first}} \leftarrow$ first event in the event sequence in \mathcal{G} associated with c
- 4: $paths \leftarrow$ depth_first_search_all_paths($\mathcal{G}, e_c^{\text{first}} \rightarrow e_t^{\text{target}}$)
- 5: **if** $paths \equiv \emptyset$ **then**
- 6: continue
- 7: **end if**
- 8: **for each** $path \in paths$ **do**
- 9: $h \leftarrow$ first event of interactions of c and a dynamic object partner
- 10: **if** $h \equiv \emptyset$ **then**
- 11: $h \leftarrow$ first in the event chain associated with c
- 12: **end if**
- 13: **if** $h \notin H$ **then**
- 14: add h to H
- 15: **end if**
- 16: **end for**
- 17: **end for**

3.2.1 CARVE dataset

We aim at building a large scale dataset with clean videos and clear causal relationships that can be used to validate the hypotheses and verify core operation of methods. To generate the videos, we utilize the 2D physics simulator provided by [16] to generate complex dynamic physical interactions of 2D objects. We generate 10K videos with over 250K abductive event pairs of target and trigger events. The videos and their abductive event pairs are divided into train, validation and test split with a ratio of 60:20:20.

Video generation: The videos are 10 seconds long of 256×256 pixel resolutions. They are created from 20 pre-defined scenes with physical interactions of *dynamic objects* and *static scene elements*. There are 48 variants of dynamic objects derived by selecting among 2 sizes (small, large), 3 shapes (cube, triangle, circle) and 8 colors. We design 7 static scene elements (ramp, platform, button, basket, left wall, right wall and ground). Object and element positions are randomly initiated.

Dynamic object events: In this dataset, we specify video events based on the interactions of objects, named *dynamic-object events*. We first track the movement of each object and detect its *state changes* caused by *interactions* with other objects by looking for sudden changes in velocity or direction of its movement. We then match the pairs of state changes of two objects happening within the proximal time and space to locate the interactions. The *interaction* is classified into two types of *collision* and *slide*. For interactions involving more than two objects, we break them into different combinations of two-object interactions.

The event is specified by its start and end times indicating *the time interval between two consecutive collisions that result in a change in the main object’s movement direction*. The event feature vector is then form as: $\langle object_id_1, object_id_2, interaction_type, start_time, end_time \rangle$.

To form the relational structure of the events, we build a directed graph $\mathcal{G} = (\mathcal{V}, \mathcal{E})$ of dynamic-object events, where the nodes \mathcal{V} represents events and the edges \mathcal{E} represent the temporal order between them. Within the graph \mathcal{G} , for each object, we obtain a set of *chain of events* through that object’s lifeline throughout the course of a video. These event chains intersect at the events that involve two dynamic objects. See Figure 1 for an illustration .

Generating Trigger-target event pairs:

For each original video, we generate a *counterfactual variant* by removing a dynamic object at the beginning of the original video and re-running simulation. We then pick one event from the event graph of the original video as a target event; and then try to search for the existence of the target event in a counterfactual video graph by similar object attributes and time-space location. If the target event is not found in the counterfactual video, the removed dynamic object is marked as *affecting* the event. In contrast, if no match is found, we say the removed object to be *non-affecting* of the target event.

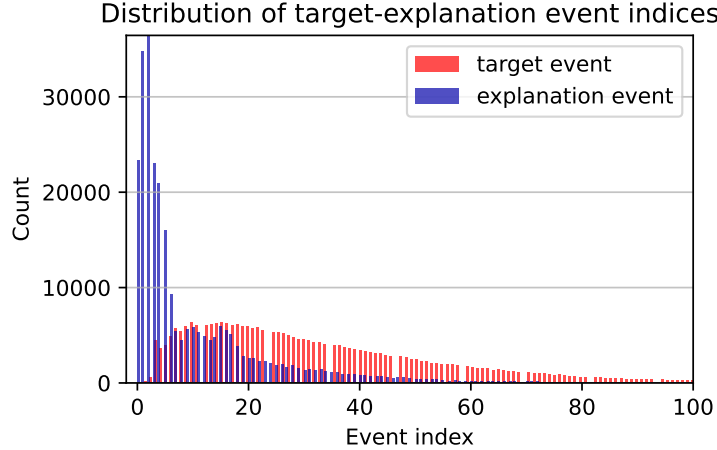


Figure 2: Distribution of target and trigger event locations in time in CARVE. Only 100 first events are visible.

For each affecting object of the target event, we identify the first event involving a dynamic object partner in its event chain as a possible trigger event. This means *a single target event may have multiple trigger events, depending on the number of affecting objects involved*. If no event involving a dynamic object partner exists, the first event in the chain is chosen (See Algorithm 1). This procedure is repeated for all possible target events of the original video graph. We note that target and trigger events do not necessarily share a common dynamic object. Instead, the target event can be an end result of a series of collisions via multiple intermediate objects, which is initiated by the trigger event.

Data splits and statistics: After discarding 9 videos where no abductive event pairs, the remaining videos are divided into 3 splits: *train*, *validation* and *test*, with a ratio *60:20:20*. This results in a large-scale dataset of a total 254,278 pairs where the train, validation and test split take 152,916 pairs, 50,822 pairs and 50,540 pairs, respectively.

Figure 2 shows the distributions of target and trigger event locations in our CARVE dataset. This graph shows that the trigger events are neither simply the first event in a chain nor the event right before the target event, instead they can be any preoccurring events. This quality of data prevent ML models from tactically remembering heuristics and requires them to properly discover the event causal relations.

3.2.2 The EpicKitchen-AR Dataset

While CARVE is clean with strong trigger-target relations, we would like to extend the benchmark to *real-world videos* where these relations are naturally entangled with other types of relations and environmental factors. To this end, we employ the Epic-Kitchen-100 [35], a major dataset originally designed for action forecasting task. This task involves predicting an action starting at a particular time based on a sequence of past event observations.

To upgrade Epic-Kitchen to an Abductive reasoning dataset, we need to generate a set of trigger-target event pairs for the video. This is a big challenge because unlike CARVE, we cannot create counterfactual videos to determine the trigger event for the target. To overcome this challenge, we leverage the current state-of-the-art action anticipation method, AFFT [36], as an oracle model to generate pseudo-counterfactual trigger-target pairs.

The process starts by running the action prediction oracle on all videos and selecting ones where the oracle model produces correct top-5 action predictions. Next, we join adjacent actions with the same label into events. We then consider the target event to be the event that contains the predicted action. The pseudo-counterfactual process is done by masking out each past event in the observation sequence one-by-one to observe changes in the oracle prediction of the target event. Now with these hypothetical event sequences, similarly to CARVE dataset, we define a trigger event to be the first event whose ablation causes a false prediction of the target event. These trigger-target event pairs constitute our EpicKitchen-AR dataset consisting of 1,259 abductive event pairs, each found in one distinct video clip. We then use 1,000 videos for training and the remaining 259 videos for validation.

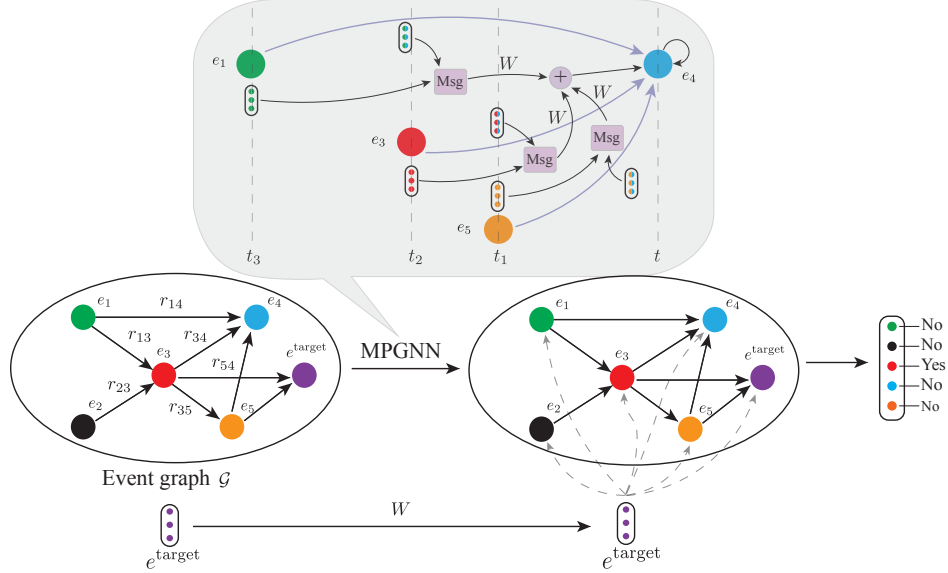


Figure 3: Overview of CERN. Given a target event e^{target} and its premise events, we build a directed graph of events \mathcal{G} based on their temporal distance. Edge feature vectors r_{ij} (arrows) represent multi-aspect relations between events. We use a novel message passing scheme (Msg) to refine events in consideration of their surrounding events. Gray box illustrates how event e_4 receives information from preceding events e_1, e_3, e_5 to refine its representation. Refined event features are then bound with the target event and eventually mapped into scores for label prediction.

4 Causal Event Relation Networks

In this section, we attempt to solve the CARVE by devising *Causal event relation network* (CERN), a neural framework that analyzes event temporal-semantic graph to quantify the trigger-target relationships. The overall architecture is demonstrated in Figure 3.

4.1 Event Representation

We aim at designing a generic model that supports a wide variety of event representation vectors e_i . The particular process to generate e_i is up to the characteristics of the dataset. For the CARVE dataset, we define an event as the interaction of two objects within a time interval between two collisions. For an event e_i , we denote x_m and x_p to be the aggregated dynamic attributes (color, shape, position etc.) of the main and partner objects during the course of the event; and ts and te be the start and end times. They stack up to form the event representation vector e_i :

$$e_i = \langle [x_m, x_p], [ts, te] \rangle. \quad (2)$$

Differently, for EpicKitchen-AR, event representation e_i is a composition vector including spatio-temporal visual features of the segments extracted using the TSN networks [36], embeddings of the action label using DistillBERT [37], and event timestamps.

4.2 Temporal-Semantic Event Graphs

Given the event sets \mathcal{V} , our objective is to model their causal relationship through building a graph-based representation multi-relational graph $\mathcal{G} = (\mathcal{V}, \mathcal{E} = \{\mathcal{E}^{\text{temp}}, \mathcal{E}^{\text{sem}}\})$. Here the edges \mathcal{E} capture not only their temporal relations $\mathcal{E}^{\text{temp}}$ but also their semantic relations \mathcal{E}^{sem} . These two types of edges are formed in the process described in this section.

Event temporal relations $\mathcal{E}^{\text{temp}}$: Considering two events e_i and e_j as defined by Eq. (2) from the event set \mathcal{V} , their temporal relationship r_{ij}^{temp} is determined based on their order in time. This can be quantified using their temporal distance $d(e_i, e_j)$ [38] which is calculated solely based on their start and end times. Assuming that the event e_i occurs during time interval $[ts_i, te_i]$ and event e_j during $[ts_j, te_j]$, their temporal distance is defined by:

$$d(e_i, e_j) = \{ts_j - ts_i, te_j - te_i, ts_j - te_i, te_j - ts_i\}. \quad (3)$$

We use Allen’s interval algebra [39] to determine the temporal relations between e_i and e_p and identify their order in time. Fundamentally, if $ts_i > ts_j$ then e_i is considered happening before e_j , denoted as $(e_i, e_j)_{i < j}$. If $ts_i = ts_j$ then end times will be considered. Details on this order rules are provided in the Supplementary. This temporal order forms the direction of edges in graph \mathcal{G} . We also use the temporal distance Eq. (3) to assign edge weights. We now have a weighted directed graph $\mathcal{G}(\mathcal{V}, \mathcal{E}^{\text{temp}})$ where information flow obeys the time order of video data in which only prior events can trigger the occurrence of later events but not in the reversed direction.

Event semantic relations \mathcal{E}^{sem} : In addition to being temporally related, events are also connected by their semantic associations. These relations are formed by the input event representation of dimension d that is created accordingly in each dataset (such as Eq. (2) for For CARVE dataset). As event relations are naturally multi-dimensional event relations (for example “force” and “direction” in object interaction), we use a k -dimensional vector $r_{e_i e_p}^{\text{sem}} \in \mathbb{R}^k$ to represent the semantic edge features. This is an improvement from the common practice of studies using scalar pairwise structural relationships [40, 41, 42]. The feature is formed by a bilinear operator:

$$r_{e_i e_j}^{\text{sem}} = \phi(e_i, e_j) \quad (4)$$

$$= \gamma_{ij} * \tanh\left(e_i^\top W^{[1:k]} e_j + b\right), \quad (5)$$

where $\gamma_{ij} \in [0, 1]$ is a distance-based penalty factor of temporal distance with detailed formulation is provided in Supp. $W^{[1:k]} \in \mathbb{R}^{d \times d \times k}$ and $b \in \mathbb{R}^k$ are learnable parameters. The bilinear operator is used on the basis of each slice of the tensor $W^{[1:k]}$ ($k \equiv d$ in our implementation).

Finally, we combine the two attributes of event relations to output a directed graph structure $\mathcal{G}(\mathcal{V}, \mathcal{E})$ representation of V nodes of an input video:

$$r_{ij} = r_{ij}^{\text{temp}} * r_{ij}^{\text{sem}}; \mathcal{E} = \{r_{ij}\}_{i=1, j=1}^V. \quad (6)$$

4.3 Abductive Reasoning on Event graphs

This section describes the learning-to-reason process on the event graphs toward finding trigger events for the targets to solve the task CARVE in Eq. (1). Given the trigger event groundtruth e_i of a target event e_t within its premise events $E(e_t) = \mathcal{G}(\mathcal{V} = \{v_i\}_{i < t}, \mathcal{E} = \{r_{ij}\}_{i, j < t})$, solving Eq. (1) becomes maximizing

$$P(y = 1 | e_t, e_i, E(e_t); \theta). \quad (7)$$

In our framework, we estimate this probability using an inference procedure using a classifier $f_\theta(\cdot)$ on top of the embeddings of target event $z_t = q_\theta(e_t)$ and trigger event candidates $h_i = p_\theta(e_i, E(e_t))$:

$$P(y = 1 | e_t, e_i, E(e_t)) = f_\theta(h_i, z_t). \quad (8)$$

In our implementation, classifier $f_\theta(\cdot)$ is a logistic classifier using concatenated $[h_i, z_t]$ as input. The target embedding function $q_\theta(e_t)$ is a linear transformation. Especially, the candidate representation learning $p_\theta(e_i, E(e_t))$ is implemented as a novel message passing scheme with L layers composed of two phases:

Message aggregation with skip connections:

$$\begin{aligned} \mathcal{F}_i^{\text{layer}}(h_i^{l-1}) &= \frac{W_1^{l-1}}{|N(i)|} \left(\sum_{j \in N(i)} \mathcal{F}_j^{\text{msg}}((h_j^{l-1}, r_{ji})) \right) + \\ &\frac{W_2^{l-1}}{|N(i)|} \sum_{j \in N(i)} (h_j^{l-1} + r_{ji}), \end{aligned} \quad (9)$$

$$\mathcal{F}_j^{\text{msg}}((h_j^{l-1}, r_{ji})) = \text{ReLU}(W_3^{l-1} [h_j^{l-1}, r_{ji}]); h_j^0 = e_i, \quad (10)$$

Layer transformation with skip connections:

$$h_i^l = \text{ReLU}\left(h_i^{l-1} + W_4^{l-1} \mathcal{F}_i^{\text{layer}}(h_i^{l-1})\right), \quad (11)$$

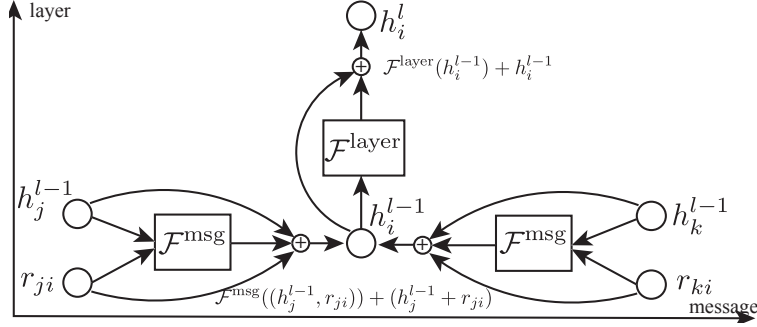


Figure 4: Message passing with skip connections along “message” and “layer” axis. \mathcal{F}^{msg} and $\mathcal{F}^{\text{layer}}$ are non-linear functions. Illustrating with two neighbors j and k of node i .

where $N(i)$ indicates neighborhood of size $|N(i)|$ of node i . W_1, W_2, W_3, W_4 are network parameters.

Unlike the standard message passing, ours uses skip connections during both message aggregation and layer transformation (Figure 4). These skip connections are of crucial roles: Those along the “message” axis offer an alternative path for information to directly flow from neighbors to node i , therefore facilitating information aggregation within a neighborhood. Meanwhile, the skip connections at the layer transformation phase create a self-loop information to update a node’s representation by itself at the current layer. As a result, it enables information from distant events to better reach later events through L layers using only single-hop neighborhood instead of having to do costly multi-hop alternatives like in [43]. Besides increasing the expressive power of the network, these skip connections also reduce gradient vanishing and facilitate training.

The network is trained end-to-end using the binary cross-entropy loss $\mathcal{L}_{\text{BCE}} = -\frac{1}{D} \sum_{i=1}^D y_i \log \tilde{y}_i + (1 - y_i) \log (1 - \tilde{y}_i)$ where D is the size of the training data and $\tilde{y}_i = f(h_i, z_t)$ indicates model predictions.

4.4 Modeling Scope and Limitation

The scope of the CARVE task and CERN model in this paper limit at endogenous causal relations, meaning that we only consider causal pairs of events that exist within a single video. This scope is relevant to vast video analysis applications such as surveillance, sport video and movie analysis. Extensions can be further made to the datasets and method to consider the out-of-video exogenous causes as hypothetical event graph nodes. Another limitation of the EpicKitchen-AR dataset is that we use an oracle event prediction model to create counterfactual causal pair. This creates a relative upper bound accuracy of the labels depending on this oracle, in contrast to the CARVE dataset where the labels are absolute through actual simulations.

5 Experiments

5.1 Data preparation

CARVE dataset: To measure efficiency together with accuracy, along with the full CARVE dataset of 10K videos and 250K+ abductive event pairs, we create two smaller subsets with the same diversity measures. Their sizes are 5K videos/80K pairs and 1K videos/18K respectively.

Toward realistic event representation, we only use object features that can be extracted from visual observation. Specifically, we use a combined feature of $2D$ positions, velocity and one-hot embeddings of static object attributes. This results in a feature vector of 71 dimensions per object, per timestep.

EpicKitchen-AR dataset: As mentioned in Section 4.1, we use spatio-temporal features of video segments as event representations which are the extracted TSN features following [36]. To enrich the event representations, we also incorporate label embeddings derived from action label annotations using DistillBERT [37].

5.2 Baselines and settings

To set the high bar for the challenge, we implement a wide set of baselines ranging from classic methods to popular modern architectures. They include *first collision*, *direct node embeddings*, *LSTM* [44], *BiLSTM* [45], *Transformer* [46], and *Video-LLaVA* [5]. The *first collision* baseline always predicts the first collision in video input as the trigger

Model	Val. Accuracy (%)			Test Accuracy (%)		
	1K	5K	10K	1K	5K	10K
Rand. guess	0.60	0.60	0.60	0.60	0.60	0.60
First collision	8.72	8.72	8.72	9.30	9.30	9.30
Node embs	18.92	25.66	32.36	18.08	27.65	32.62
LSTM	29.29	31.22	38.03	27.17	33.62	38.42
BiLSTM	28.21	32.06	38.02	27.42	34.15	37.90
Transformer	24.36	31.73	41.28	23.29	34.24	41.75
CERN	32.05	37.9	44.38	30.90	40.50	43.86

Table 1: Experiments using object-centric event features on the CARVE dataset and its subsets.

event. The *node embeddings* baseline makes prediction of about trigger events solely based on their features without considering their relations. For sequential models such as LSTM and BiLSTM, we first sort all the events localized from an input video by their start times then treat them as input sequences. To assure fairness, we conduct experiments with the popular large video-language model Video-LLaVA only on EpicKitchen-AR because they were trained with only real-world videos and language descriptions, which are not available in the visual-only CARVE dataset. See Supp. for more details on these settings.

Compared to these baselines is our *Causal event relation network* (CERN) using a 4-layer message passing framework for experiments with the CARVE dataset and 2-layer for the EpicKitchen-AR by default. These relatively deep graph structure allow the model to reach information from events living further in the past. They are possible thanks to the skip connections that avoid gradient vanishing issues.

5.3 Results on CARVE dataset

We compare the effectiveness of CERN against the baselines by feeding them the same object-centric event features in Eq. (2). The results (given in Table 1) confirm that the task cannot be solved by either making random predictions or selecting the first collision in video input as the explanation event. We also observe that BiLSTM does not offer any benefits compared to LSTM but rather degrades the performance with the backward information in some cases (37.90% vs. 38.42% on test split). This suggests that for this task, information strictly flows from past events to later events, verifying our inductive bias used in designing CERN.

Among the baselines, Transformer is the closest to our event graph network since both methods model the pairwise relationships between events. However, Transformer is less sample efficient hence, struggling to generalize with data scarcity. Our CERN model further benefits from the explicit use of the temporal orders of events and their distance in time, clearly outperforming Transformer in these experiments. This advantage is even more significant in experiments with limited training data (1K and 5K).

5.3.1 Ablation studies and analysis:

We justify the roles of CERN’s components by a series of ablation studies (Table 2):

Replacing event representations:

Without object-centric event representations: When replacing object-centric features with generic video features using a large-scale video representation MViTv2 [4] pretrained on Kinetics-400 [47]. This is the current SoTA model across different image and video understanding tasks. These features are also combined with event timestamps to make sure it is a fair comparison. Table 2 shows that using objectless features significantly degrades CERN’s performance on CARVE by over 47.0%.

Fine-tuning large video recognition models: To further verify the importance of object-centric representation and temporal information of events in learning, we fine-tune the MViTv2 models (S and B) to learn the mapping from video features to event features without providing event timestamps. Table 2 indicates that increasing both model size and training data do not enhance the model’s ability to localize events in time. This demonstrates their limitations in detecting subtle object movements and distinguishing object-centric motions essential for event representations.

Ablating model’s components:

We ablate each relation from the full CERN and observe the impacts on the performance. In details:

Experiment	Component	Val. Acc (%)
Replacing event features	MViTv2-S feats with event timestamps	23.26 (\downarrow 47.5%)
	MViTv2-S feats w/o event timestamps (finetuned)	5.89 (\downarrow 86.7%)
	MViTv2-B feats w/o event timestamps (finetuned)	5.65 (\downarrow 87.2%)
Ablating model’s components	Only temp. relations	27.46 (\downarrow 38.1%)
	Only sem. relations	40.27 (\downarrow 9.3%)
	2-layer msg passing	42.90 (\downarrow 3.3%)
	W/o msg skip connections	42.05 (\downarrow 5.2%)
	W/o layer skip connections	41.93 (\downarrow 5.5%)
	W/o skip connections	41.20 (\downarrow 7.2%)
	W/o distance penalty	40.41 (\downarrow 8.9%)
Full model		44.38

Table 2: Ablation studies and analysis on CARVE dataset. \downarrow indicates performance drop from the full model.

Model	Val. Accuracy (%)		
	Visual	Label	Combined
Rand. guess	5.56	5.56	5.56
Node embs	6.59	39.77	41.47
LSTM	33.33	45.17	45.74
Transformer	32.56	45.17	42.25
Video-LLaVA (zero-shot)	NA	NA	4.26
Video-LLaVA (in-context)	NA	NA	34.50
CERN	37.2	46.90	47.29

Table 3: Experiments on the EpicKitchen-AR dataset.

Temporal relations $\mathcal{E}^{\text{temp}}$ shows its critical roles when its ablation creates a significant drop of 38.1%/36.5% on val/test split. Similarly, only *semantic relations* \mathcal{E}^{sem} does not work well alone either, with a drop of around 9.0%.

With message passing of 2 layers instead of 4 as default, the performance dropped by 3.0%. More importantly, the *Message skip connections* shows their roles as ablating them has a bigger negative impact on the performance of around 5.0%. Similarly, when we remove the direct connections h_i^{l-1} , the performance also drops over 5.0%. Together, *Ablating all skip connections* (Eqs. (9-11)) results in a combined degradation by around 7.0%.

Finally, when we remove the *distance penalty in event relations* (γ_{ip} factor in Eq. (4)), we see a major effect of performance drop of 8.9%/8.6% on val/test sets.

5.4 Results on EpicKitchen-AR:

We compare the performance of CERN against the baselines on EpicKitchen-AR, examining different types of event representations, including visual embeddings, label embeddings and combined embeddings of the features (Table 3). We particularly compare to the popular multi-purpose large video-language model Video-LLaVA [5] where it has access to language descriptions (event labels), to maximize its capabilities. We tried both zero-shot and in-context learning settings. For zero-shot, we instruct Video-LLaVA to select the trigger among the set of premise events for a target event and match its generated responses to ground-truth events. In the in-context setting, each test sample is accompanied by two examples with the target-trigger annotations from the train set as in-context samples. Details of the prompts used are provided in the Supplementary.

Table 3 shows that *CERN clearly outperforms the baselines for all of the cases* with visual-only, label-only and combined visual-label event representations. Interestingly, the direct node embeddings baseline completely failed to

find trigger events in visual-only case, suggesting event visual representations are highly complex and requires stronger modeling capability. Most notably, Video-LLaVA struggled to understand the causal relationships between events, highlighting the lack of reasoning ability despite its capacity to generate plausible text descriptions about video contents. Our proposed method CERN also *consistently outperforms LSTM and Transformer*. It is to note that Transformer gets 3.0% performance drop in the combined case compared to label-only. This is explainable as Transformer is known to be data hungry and could not generalize with the available data to make visual feature useful.

While setting the state of the art, the performances of CERN and other baselines are still far from perfect at the CARVE task on both datasets, suggesting *an open playground for future works* in this new task.

6 Discussion

This paper promotes the task of Causal Abductive Reasoning on Video Events (CARVE), an important but under-explored AI capability. The task is supported by two new benchmark datasets with clean and realistic videos created using our counterfactual synthesis procedures. We also introduced the Causal Event Relation Networks (CERN), a new neural framework operating on event graph can learn to effectively find the trigger events in videos. While CERN outperforms many baselines, including finetuned large-scale generic models, the new task is proved to be highly challenging and calling for further advances toward causal abductive reasoning for visual data.

References

- [1] Kaiming He, Xiangyu Zhang, Shaoqing Ren, and Jian Sun. Delving deep into rectifiers: Surpassing human-level performance on imagenet classification. In *ICCV*, pages 1026–1034, 2015. 1
- [2] Yannis M Assael, Brendan Shillingford, Shimon Whiteson, and Nando De Freitas. Lipnet: End-to-end sentence-level lipreading. *ICLR*, 2017. 1
- [3] Charles Sanders Peirce. *Collected papers of Charles Sanders Peirce*, volume 5. Harvard University Press, 1974. 1
- [4] Yanghao Li, Chao-Yuan Wu, Haoqi Fan, Karttikeya Mangalam, Bo Xiong, Jitendra Malik, and Christoph Feichtenhofer. Mvitv2: Improved multiscale vision transformers for classification and detection. In *CVPR*, pages 4804–4814, 2022. 1, 2, 5.3.1
- [5] Bin Lin, Yang Ye, Bin Zhu, Jiayi Cui, Munan Ning, Peng Jin, and Li Yuan. Video-llava: Learning united visual representation by alignment before projection. *arXiv preprint arXiv:2311.10122*, 2023. 1, 5.2, 5.4, B.2
- [6] Anoop Cherian, Chiori Hori, Tim K Marks, and Jonathan Le Roux. (2.5+ 1) d spatio-temporal scene graphs for video question answering. In *Proceedings of the AAAI Conference on Artificial Intelligence*, volume 36, pages 444–453, 2022. 2
- [7] Long Hoang Dang, Thao Minh Le, Vuong Le, and Truyen Tran. Hierarchical object-oriented spatio-temporal reasoning for video question answering. *IJCAI*, 2021. 2
- [8] Kexin Yi, Chuang Gan, Yunzhu Li, Pushmeet Kohli, Jiajun Wu, Antonio Torralba, and Joshua B. Tenenbaum. CLEVRER: CoLLision Events for Video REpresentation and Reasoning. In *ICLR*, 2020. 2, 3.1, 3.2
- [9] Difei Gao, Luwei Zhou, Lei Ji, Linchao Zhu, Yi Yang, and Mike Zheng Shou. Mist: Multi-modal iterative spatial-temporal transformer for long-form video question answering. In *Proceedings of the IEEE/CVF conference on computer vision and pattern recognition*, pages 14773–14783, 2023. 2
- [10] Chen Liang, Wenguan Wang, Tianfei Zhou, and Yi Yang. Visual abductive reasoning. In *Proceedings of the IEEE/CVF Conference on Computer Vision and Pattern Recognition*, pages 15565–15575, 2022. 2, 3.1, 3.2
- [11] Wenliang Zhao, Yongming Rao, Yansong Tang, Jie Zhou, and Jiwen Lu. VideoABC: A Real-World Video Dataset for Abductive Visual Reasoning. *IEEE Transactions on Image Processing*, 31:6048–6061, 2022. 2
- [12] Jack Hessel, Jena D Hwang, Jae Sung Park, Rowan Zellers, Chandra Bhagavatula, Anna Rohrbach, Kate Saenko, and Yejin Choi. The abduction of sherlock holmes: A dataset for visual abductive reasoning. In *ECCV*, pages 558–575. Springer, 2022. 2
- [13] Jakob Suchan, Mehul Bhatt, Przemysław Wałęga, and Carl Schultz. Visual explanation by high-level abduction: On answer-set programming driven reasoning about moving objects. In *AAAI*, volume 32, 2018. 2

- [14] Yunzhu Li, Antonio Torralba, Animashree Anandkumar, Dieter Fox, and Animesh Garg. Causal discovery in physical systems from videos. *Neural Information Processing Systems (NeurIPS)*, 2020. 2
- [15] Mingyu Ding, Zhenfang Chen, Tao Du, Ping Luo, Josh Tenenbaum, and Chuang Gan. Dynamic visual reasoning by learning differentiable physics models from video and language. *NeurIPS*, 34:887–899, 2021. 2
- [16] Tayfun Ates, M Samil Atesoglu, Cagatay Yigit, Ilker Kesen, Mert Kobas, Erkut Erdem, Aykut Erdem, Tilbe Goksun, and Deniz Yuret. Craft: A benchmark for causal reasoning about forces and interactions. *ACL*, pages 2602–2627, 2022. 2, 3.2.1
- [17] Francesco Locatello, Dirk Weissenborn, Thomas Unterthiner, Aravindh Mahendran, Georg Heigold, Jakob Uszkoreit, Alexey Dosovitskiy, and Thomas Kipf. Object-centric learning with slot attention. *NeurIPS*, 33: 11525–11538, 2020. 2
- [18] Rohit Girdhar and Deva Ramanan. Cater: A diagnostic dataset for compositional actions and temporal reasoning. *arXiv preprint arXiv:1910.04744*, 2019. 2
- [19] Jiayuan Mao, Xuelin Yang, Xikun Zhang, Noah Goodman, and Jiajun Wu. CLEVRER-Humans: Describing Physical and Causal Events the Human Way. In *NeurIPS Datasets and Benchmarks Track*, 2022. 2, 3.1, 3.2
- [20] Xiaolong Liu, Yao Hu, Song Bai, Fei Ding, Xiang Bai, and Philip HS Torr. Multi-shot temporal event localization: a benchmark. In *CVPR*, pages 12596–12606, 2021. 2
- [21] Xiyang Dai, Bharat Singh, Guyue Zhang, Larry S Davis, and Yan Qiu Chen. Temporal context network for activity localization in videos. In *ICCV*, pages 5793–5802, 2017. 2
- [22] Kun Xia, Le Wang, Sanping Zhou, Nanning Zheng, and Wei Tang. Learning to refactor action and co-occurrence features for temporal action localization. In *CVPR*, pages 13884–13893, 2022. 2
- [23] Jie Lei, Licheng Yu, Tamara L Berg, and Mohit Bansal. What is more likely to happen next? video-and-language future event prediction. *EMNLP*, pages 8769–8784, 2020. 2
- [24] Jae Sung Park, Chandra Bhagavatula, Roozbeh Mottaghi, Ali Farhadi, and Yejin Choi. Visualcomet: Reasoning about the dynamic context of a still image. In *ECCV*, pages 508–524. Springer, 2020. 2
- [25] Jingwei Ji, Ranjay Krishna, Li Fei-Fei, and Juan Carlos Niebles. Action genome: Actions as compositions of spatio-temporal scene graphs. In *CVPR*, pages 10236–10247, 2020. 2
- [26] Arka Sadhu, Tanmay Gupta, Mark Yatskar, Ram Nevatia, and Aniruddha Kembhavi. Visual semantic role labeling for video understanding. In *CVPR*, pages 5589–5600, 2021. 2
- [27] Hammad A Ayyubi, Christopher Thomas, Lovish Chum, Rahul Lokesh, Yulei Niu, Xudong Lin, Long Chen, Jaywon Koo, Sounak Ray, and Shih-Fu Chang. Multimodal event graphs: Towards event centric understanding of multimodal world. *arXiv preprint arXiv:2206.07207*, 2022. 2
- [28] Anurag Arnab, Mostafa Dehghani, Georg Heigold, Chen Sun, Mario Lučić, and Cordelia Schmid. Vivit: A video vision transformer. In *ICCV*, pages 6836–6846, 2021. 2
- [29] Ze Liu, Jia Ning, Yue Cao, Yixuan Wei, Zheng Zhang, Stephen Lin, and Han Hu. Video swin transformer. In *CVPR*, pages 3202–3211, 2022. 2
- [30] Marc Denecker, Lode Missiaen, and Maurice Bruynooghe. Temporal reasoning with abductive event calculus. In *ECAI*, pages 384–388. John Wiley and Sons; Chichester, 1992. 2
- [31] Chandra Bhagavatula, Ronan Le Bras, Chaitanya Malaviya, Keisuke Sakaguchi, Ari Holtzman, Hannah Rashkin, Doug Downey, Scott Wen-tau Yih, and Yejin Choi. Abductive commonsense reasoning. *ICLR*, 2019. 2
- [32] Corinna Elsenbroich, Oliver Kutz, and Ulrike Sattler. A case for abductive reasoning over ontologies. In *OWLED*, volume 216, 2006. 2
- [33] Joerg Schoenfish, Christian Meilicke, Janno von Stülpnagel, Jens Ortmann, and Heiner Stuckenschmidt. Root cause analysis in it infrastructures using ontologies and abduction in markov logic networks. *Information Systems*, 74:103–116, 2018. 2

- [34] Judea Pearl et al. Causality: Models, reasoning and inference. *Cambridge, UK: CambridgeUniversityPress*, 19, 2000. 3.2
- [35] Dima Damen, Hazel Doughty, Giovanni Maria Farinella, Antonino Furnari, Evangelos Kazakos, Jian Ma, Davide Moltisanti, Jonathan Munro, Toby Perrett, Will Price, et al. Rescaling egocentric vision: Collection, pipeline and challenges for epic-kitchens-100. *International Journal of Computer Vision*, pages 1–23, 2022. 3.2.2
- [36] Zeyun Zhong, David Schneider, Michael Voit, Rainer Stiefelhagen, and Jürgen Beyerer. Anticipative feature fusion transformer for multi-modal action anticipation. In *Proceedings of the IEEE/CVF Winter Conference on Applications of Computer Vision*, pages 6068–6077, 2023. 3.2.2, 4.1, 5.1
- [37] Victor Sanh, Lysandre Debut, Julien Chaumond, and Thomas Wolf. Distilbert, a distilled version of bert: smaller, faster, cheaper and lighter. *NeurIPS*, 2019. 4.1, 5.1
- [38] Yongmian Zhang, Yifan Zhang, Eran Swears, Natalia Larios, Ziheng Wang, and Qiang Ji. Modeling temporal interactions with interval temporal bayesian networks for complex activity recognition. *TPAMI*, 35(10):2468–2483, 2013. 4.2
- [39] James F Allen. Maintaining knowledge about temporal intervals. *Communications of the ACM*, 26(11):832–843, 1983. 4.2, A.1
- [40] Anurag Arnab, Chen Sun, and Cordelia Schmid. Unified graph structured models for video understanding. In *ICCV*, pages 8117–8126, 2021. 4.2
- [41] Feng Mao, Xiang Wu, Hui Xue, and Rong Zhang. Hierarchical video frame sequence representation with deep convolutional graph network. In *ECCV workshops*, pages 0–0, 2018. 4.2
- [42] Wenguan Wang, Xiankai Lu, Jianbing Shen, David J Crandall, and Ling Shao. Zero-shot video object segmentation via attentive graph neural networks. In *ICCV*, pages 9236–9245, 2019. 4.2
- [43] Jiarui Feng, Yixin Chen, Fuhai Li, Anindya Sarkar, and Muhan Zhang. How powerful are k-hop message passing graph neural networks. *NeurIPS*, 2022. 4.3
- [44] Sepp Hochreiter and Jürgen Schmidhuber. Long short-term memory. *Neural computation*, 9(8):1735–1780, 1997. 5.2, B.2
- [45] Alex Graves and Jürgen Schmidhuber. Framewise phoneme classification with bidirectional lstm and other neural network architectures. *Neural networks*, 18(5-6):602–610, 2005. 5.2, B.2
- [46] Ashish Vaswani, Noam Shazeer, Niki Parmar, Jakob Uszkoreit, Llion Jones, Aidan N Gomez, Łukasz Kaiser, and Illia Polosukhin. Attention is all you need. *NIPS*, 30, 2017. 5.2, B.2
- [47] Will Kay, Joao Carreira, Karen Simonyan, Brian Zhang, Chloe Hillier, Sudheendra Vijayanarasimhan, Fabio Viola, Tim Green, Trevor Back, Paul Natsev, et al. The kinetics human action video dataset. *arXiv preprint arXiv:1705.06950*, 2017. 5.3.1
- [48] Diederik Kingma and Jimmy Ba. Adam: A method for stochastic optimization. *ICLR*, 2014. B.1

Supplementary material

Introduction

In this supplementary material, we provide further details on the implementation of our proposed method CERN and the baselines discussed in the Experiment section in the main paper and additional analyses. This includes:

- Additional details of CERN
- Implementation details
- Some qualitative results on the CARVE dataset

A Additional Details of CERN

A.1 Event temporal relations

$t_j^s - t_i^s$	$t_j^e - t_i^e$	$t_j^s - t_i^e$	$t_j^e - t_i^s$	Interpretation
+	+	+	+	e_i before e_j ($e_i \rightarrow e_j$)
-	-	-	-	e_j before e_i ($e_i \leftarrow e_j$)
-	+	+	-	e_i during e_j ($e_i \rightarrow e_j$)
+	-	-	+	e_j during e_i ($e_i \leftarrow e_j$)
+	+	+	-	e_i overlaps e_j ($e_i \rightarrow e_j$)
-	-	+	-	e_j overlaps e_i ($e_i \leftarrow e_j$)
+	+	+	0	e_i meets e_p ($e_i \rightarrow e_j$)
-	-	0	-	e_j meets e_i ($e_i \leftarrow e_j$)
0	+	-	+	e_i starts e_p ($e_i \rightarrow e_j$)
0	-	-	+	e_p starts e_i ($e_i \leftarrow e_j$)
-	0	-	+	e_i finishes e_j ($e_i \rightarrow e_j$)
+	0	-	+	e_j finishes e_i ($e_i \leftarrow e_j$)
0	0	any	any	e_i equals e_j ($e_i \rightarrow e_j$)

Table 4: Identifying the temporal order between event e_i and e_p based on Allen’s atomic interval temporal relations.

As mentioned in the main paper, we use Allen’s interval algebra [39] to determine the temporal relations between a pair of temporal events e_i and e_j . Specifically, given the temporal distance between the two events as in the Eq. 3 in the main paper, their order in time is determined using in Table 4. As can be seen, these orders are mainly based on the events’ start times. If the two events have the same start time, their end times will be considered.

A.2 Event semantic relations

The distance-based penalty factor of temporal distance γ_{ip} in Eq. 5 of the main paper is computed by:

$$\gamma_{ij} = \exp(-\beta * d_{ij}), \text{ where} \quad (12)$$

$$d_{ij}(e_i, e_j)_{i < j} = \sqrt{(ts_j - ts_i)^2 + (te_j - te_i)^2} \quad (13)$$

is the Euclidean distance between events e_i and e_j ; β is a learnable positive decay factor that compensates for the uncertainty in calculating the distance d_{ij} . The more distant the two events are in time, the weaker their relation is.

B Implementation Details

B.1 CERN

We implemented our proposed method CERN using DGL 0.9.1 and Pytorch 1.11.0 or later. We have experimented with up to 4 layers of message passing in which we found slight improvements when increasing the number of layers as

reported in the Experiment section in the main paper. Our proposed model is optimized using Adam optimizer [48] with initial learning rate is set to 10^{-4} . The learning rate gradually decreases at every epoch. We train a total 100 epochs with a batch size of 128 which takes approximately 18 hours on a single GPU NVIDIA A100 to finish the training on the full CARVE dataset.

B.2 Baselines

This section provides details of the baselines used in the Experiment section, which include:

First collision: This experiment aims to verify whether it is sufficient to always set the first collision detected in video input as the trigger event, regardless of the target event considered.

Node embeddings: Directly use node embeddings of the events by using a linear neural network layer. This experiment does not consider video structure and relationships of any kinds between the nodes.

LSTM [44]: We first sort all the events localized from an input video by their occurrence in time. We then simply treat them as a sequence and use LSTM networks to model the temporal relationships between the events. The output hidden states of LSTM are then used as the latent representation h_i of the events in Eq. (12) in the main paper.

BiLSTM [45]: Instead of using LSTM, we use a bidirectional LSTM variant to model the sequential relationships between events. The objective is to take advantage of signals propagating both forward and backward in time.

Transformer [46]: Similarly, we also sort all the events by their occurrence times to create a sequence of events. We implement a vanilla version of Transformer with 6 layers of self-attention to refine the representations of the events by taking into account their relationships with all other events in the sequence. We use the same parameters as suggested in the original paper in our implementation.

Video-LLaVA [5]: To evaluate whether large video-language models can comprehend the causal relationships between video events, we conduct experiments with Video-LLaVA on the EpicKitchen-AR dataset using two settings: zero-shot setting and in-context setting.

In the zero-shot setting, Video-LLaVA is instructed to respond to a templated question where it must identify the trigger event for a target event from a list of premise events. Careful instructions are provided to ensure consistent responses from Video-LLaVA. We have tried different prompts and reported the one with the best results.

In the in-context learning setting, for each sample in the test set of the EpicKitchen-AR, we provide 2 samples with groundtruth answers taken from the train set. These examples serve as context to guide Video-LLaVA's responses. The same instruction format as the zero-shot setting is used in this experiment. Specifically, the following prompt is given to Video-LLaVA :

“ USER: <video>Given a sequence of premise events include {premise_events}, what is the cause event of the event {target_event}? Choose a correct answer within the premise events. ASSISTANT:”

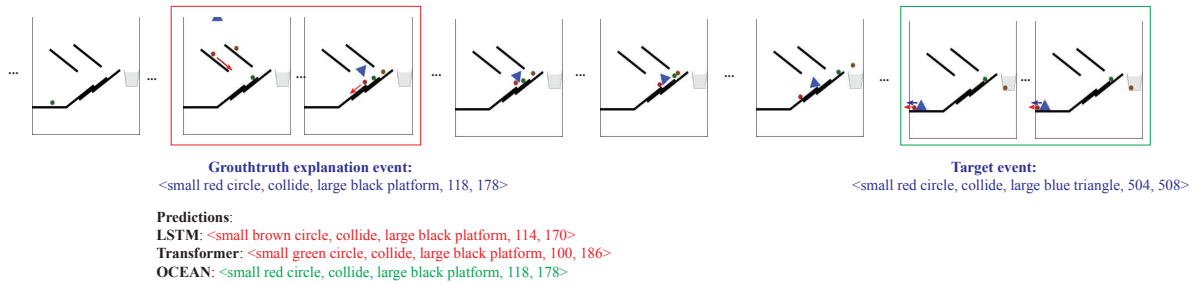
All of these baselines are implemented using Pytorch 1.11.0 or later with similar hyper-parameters as our proposed model CERN for fair comparisons.

C Analysis

Figure 5 presents typical examples where the graph structure modeled by CERN helps trace back events associated with a co-referenced object between target-trigger events to identify the correct trigger events. In contrast, LSTM and Transformer struggle to keep track of these event sequences due to their assumptions on the sequential relationships between events. Furthermore, we also observe that LSTM and Transformer often make similar mistakes in these examples as they tend to select events that occur at beginning of a video input as trigger events, thus fail to identify trigger events that locate at the middle of the video.

However, we also showcase an example where all the studied methods struggle in Figure 6. This often occurs when there are multiple concurrent events happen within a scene during the life of the trigger event. The inability of these models to handle such scenarios suggest a need for a novel approach that goes beyond the common feature association between events.

Sample 1:



Sample 2:

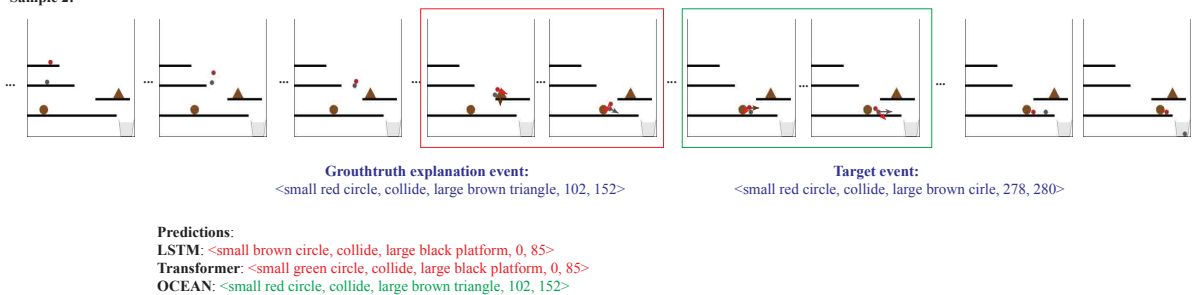


Figure 5: Qualitative examples demonstrating that sequential models struggle to identify correct trigger events while CERN handles successfully. Sequential models tend to predict events that occur early in time as the trigger events and often incapable of tracing back events associated with a co-referenced object between the target and trigger event. The graph structure learned by CERN has potential to facilitate the propagation of information along chains of events associated with dynamic objects, thereby benefiting the learning. Colored arrows indicate the direction of the movement of the corresponding objects. Best viewed in color.

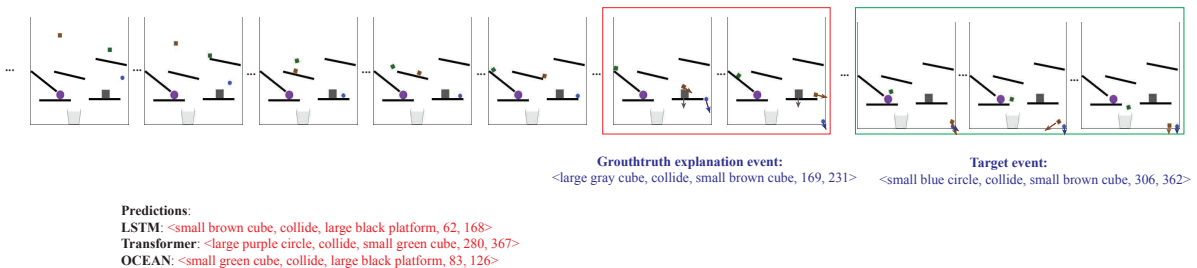


Figure 6: A showcase for the challenges of our CARVE dataset that all the studied methods struggle. This is often the case when there are multiple concurrent events occurring within the times of the trigger event. Best viewed in color.